

diffraction intensity in plane is of the order of $\frac{1}{2}\%$ of the incident beam. Strong vicinal out-of-plane peaks recorded in scans using a larger detector acceptance angle (1.4°) indicate that the total diffractive scattering may be a substantial fraction of I_0 as expected for an estimated surface Debye temperature of 360 K.⁵ There is some indication that a hard-wall potential with a weak attractive well is appropriate for this scattering system. The different structural models which have been proposed for the Si(111) 7×7 reconstruction⁷⁻⁹ are expected to generate quite different intensity sequences versus θ_r for the range of incident conditions we report. Consequently, we think that the data we present here are sufficient to give each model a critical test.

¹R. E. Schlier and H. E. Farnsworth, J. Chem. Phys.

30, 917 (1959); J. J. Lander and J. Morrison, J. Chem. Phys. 37, 729 (1962).

²Cf. W. Mönch and P. P. Auer, J. Vac. Sci. Technol. 15, 1230 (1978), and references therein.

³M. J. Cardillo, C. C. Ching, E. F. Greene, and G. E. Becker, J. Vac. Sci. Technol. 15, 423 (1978).

⁴M. J. Cardillo and G. E. Becker, Phys. Rev. Lett. 40, 1148 (1978).

⁵Assuming $\theta_D^{\text{surface}} = \frac{2}{3}\theta_D^{\text{bulk}}$, with $\theta_D^{\text{bulk}} = 543$ K [B. W. Batterman and D. R. Chipman, Phys. Rev. 127, 690 (1962)], we estimate a reduction in the total diffraction intensities to $I/I_0 = 10-20\%$, for a range of the He/Si attractive well depth of 10-20 meV.

⁶E. Grimmelmann and J. C. Tully, private communication.

⁷J. J. Lander and J. Morrison, J. Appl. Phys. 34, 1403 (1963).

⁸W. A. Harrison, Surf. Sci. 55, 1 (1976).

⁹J. D. Levine, S. H. McFarlane, and P. Mark, Phys. Rev. B 16, 5415 (1977).

Sample-Shape-Dependent Phase Transition of Hydrogen in Niobium

H. Zabel

Sektion Physik der Universität München, D 8000 München 22, Germany, and Department of Physics, University of Houston, Houston, Texas 77004^(a)

and

H. Peisl

Sektion Physik der Universität München, D 8000 München 22, Germany

(Received 13 December 1978)

The coherent $\alpha-\alpha'$ phase transition of H in Nb has been studied in several sample shapes. The samples were loaded *in situ* with the critical hydrogen concentration of 0.31 H/Nb above $T_c = 171^\circ\text{C}$ and slowly cooled. Below T_c a coherent macroscopic spinodal decomposition takes place. By x-ray scattering and examination of the relaxed crystals, the spatial arrangement of the phases was determined. The macroscopic modes so revealed depend sensitively upon sample shape through the fulfillment of the elastic boundary condition.

The $\alpha-\alpha'$ phase transition of H in Nb resembles a gas-liquid transition of a real gas.^{1,2} In this transition the lattice retains its original bcc symmetry, and the phases are only distinguishable by their different lattice expansions. This transition and similar transitions in PdH (Ref. 3) and PdAgH (Ref. 4) are still under discussion.^{5,6} They have often been treated as textbook examples of a lattice gas,^{7,8} and the interaction energy, responsible for the phase transition, is introduced as a suitable parameter proportional to the measured critical temperature T_c . In contrast to the lattice-gas model the real lattice is deformable and the interstitially dissolved protons set up long-range distortion fields.⁹⁻¹¹ The $\alpha-\alpha'$

transition has therefore been attributed to an elastic interaction via this lattice distortion induced by the protons.^{12,13} The model of elastic interaction leads in turn to the concept of macroscopic elastic modes^{14,15} caused by internal stress produced by the inhomogeneous hydrogen density variation in a coherent lattice. At T_c only a few modes become unstable which depend upon the sample geometry through the fulfillment of the elastic boundary condition. Therefore, the study of the shape dependence of the phase transition is a crucial test of the validity of the elastic interaction as the main contribution to the attractive part of the energy.

Nb samples (single crystals, wires, and foils)

were purchased from Materials Research Corporation with a stated purity of 99.98%. A single-crystal rod with diameter of 12.5 mm and [110] orientation was cut in several slices with thicknesses of 0.3, 0.6, 2, and 10 mm. Wires of diameter 0.25, 0.76, and 1.2 mm were cut in pieces of 13 mm length. The foil had an average thickness of 100 μm . The samples were out-gassed at 2200°C for several hours in a vacuum of 10^{-10} Torr. They were then mounted in a special high-temperature x-ray furnace designed to permit the *in situ* loading with hydrogen. This was accomplished by first heating to about 600°C in a vacuum of 10^{-7} Torr. Then hydrogen, purified by a Pd cell, was introduced. The dissolved hydrogen concentration was determined simultaneously by continuously monitoring the lattice parameter. After reaching the critical concentration, the sample was cooled slowly to the vicinity of the critical point [$c_c = 0.31$ H/Nb, $T_c = 171^\circ\text{C}$ (Ref. 16)]. This *in situ* loading procedure is essential to establish well-defined initial conditions for a coherent lattice. Below 400°C an

oxygen layer at the surface seals the sample and assures an isochoral study of the phase transition. Special holders for the different sample shapes allowed them to relax freely under the constraint of internal sample stresses. The entire furnace was rotatable in order to scatter x rays from different parts of the sample. We used a standard x-ray scattering geometry for $\theta:2\theta$ scans, with a commercial 1.2-kW x-ray generator, Mo tube, and diffractometer. Scanning electron micrographs (SEM) were taken at 50 \times to 100 \times magnification.

The results¹⁷ of the shape dependence of the coherent α - α' phase transition are summarized in Fig. 1. The original shape in each of the sample geometries studied is sketched in the first line at the top. The second line contains photographs or SEM pictures of the samples at room temperature and the last (fourth) line reproduces x-ray measurements of the lattice parameters during the cooling run immediately following *in situ* hydrogen loading. In the third line two-dimensional density profiles are outlined as a

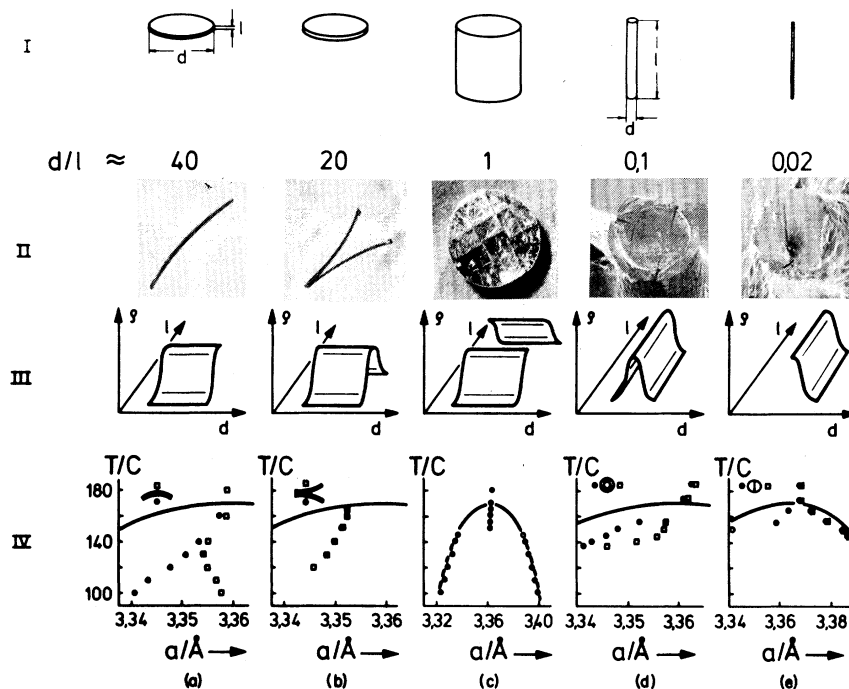


FIG. 1. Sample-shape dependence of macroscopic hydrogen density modes due to coherent phase transition α - α' . (a) 0.3-mm-thick disk-shaped single crystal, (b) 0.6-mm-thick disk-shaped single crystal, (c) 2- to 10-mm-thick disks, (d) 1.2-mm-diam wire, (e) 1.76- to 0.25-mm-diam wires. Horizontal designations are (I) initial sample geometry, (II) room-temperature photographs following final measurements [in (IV)], (III) two-dimensional density profiles of the hydrogen fluctuation, (IV) lattice parameter vs temperature taken on different parts of the samples as indicated by the insets. Full lines represent the incoherent α - α' phase boundary.

result of both the second and the fourth lines. In the first example [Fig. 1(a)] the lattice parameters were measured alternately on both sides of a 0.3-mm-thick disk-shaped Nb single crystal. The lattice parameters exhibit the same temperature-dependent shift above T_c down to the incoherent phase boundary. Below the phase boundary they do not follow the incoherent phase separation, denoted by the solid line which was determined in a companion study of the incoherent phase boundaries.¹⁷ Finally at $T \approx 150^\circ\text{C}$, the lattice parameters move apart toward the outer boundary. Following this sequence the crystal was bent like a spherical shell. The smaller lattice parameter was measured at the inner contracted plane and the larger lattice parameter at the opposite expanded surface. A hydrogen density distribution which is consistent with the bending and the measured lattice parameters has to vary macroscopically between the top and bottom plane of the disk from low to high densities as in line III. In the second example [Fig. 1(b)] a doubly thick disk-shaped crystal was chosen and the same measurements were carried out as in Fig. 1(a). Here the lattice parameters show a parallel course even within the miscibility gap below the incoherent phase boundary. This crystal was subsequently shown to be split through the middle parallel to the disk plane. The thickness and bending radius of either part are almost the same as in the first example. Thus the relaxation of the crystal and the lattice-parameter measurement suggest a macroscopic hydrogen density fluctuation which varies smoothly from low density on one surface to high density in the middle, and back to low density on the opposite surface. The fluctuation wave thereby represents a full-wavelength density mode in contrast to the half-wavelength mode of the first example. In still thicker disks (cylinders) with otherwise the same diameter, invariably the lower-density α phase was detected at the outside. Small slices with similar thickness and bending radius were often split or fractured over the surface [Fig. 1(c)]. It is supposed that in the inner parts of the crystal more complex density distributions occur, because of the constraint of the neighboring layers. Thus they cannot relax in the same manner as before. The constrained condition was simulated by a 0.1-mm-thick foil, squeezed in the sample holder so as to restrict the bending or freedom to relax under the macroscopic deformation. The resultant T versus a diagram in Fig. 1(c) shows that the density distribution stays

constant to 20 deg below T_c , followed by a sudden, incoherent, phase separation. From the intensity of the Bragg reflections, it can be concluded that the phases are distributed equally in the foil plane in this externally constrained sample.

Wires of 1.2-mm diam [Fig. 1(d)] exhibit a cylindrically symmetric precipitation structure, as can be seen by the SEM photograph. A lattice-parameter check showed that the α' phase is located in the core of the wire, surrounded by the α phase in the cylinder wall. Thus, the spatial arrangement of the phases is generated by a full-wavelength density fluctuation normal to the wire axis, similar, say, to a drum mode. In the last example of 0.76- to 0.25-mm-thick wires [Fig. 1(e)] the phases α and α' precipitate in a half-cylindrical symmetry, i.e., each half-cylinder is occupied by one of the phases, either α or α' .

The photographs in Fig. 1 clearly exhibit an incoherent state of the crystals. However, they are frozen pictures of the original coherent density fluctuations, and thus demonstrate, together with the x-ray scattering experiments, the spatial arrangement of the early-stage coherent spinodal decomposition below T_c . The coherent phase transition is defined by a continuous variation of lattice parameter due to a spatially continuous variation of hydrogen concentration, while the incoherent phase transition shows a mismatch of lattice parameters at the interface of the phases α and α' . Our view of the sequence presented is as follows: Inhomogeneous density fluctuations below T_c set up inhomogeneous lattice distortions, which create so-called coherency stresses. At a certain temperature below T_c , they may exceed the critical shear stress for the onset of plastic deformation. At this point, dislocations and cracks, generated by further cooling, decorate those parts of the crystals which contained the highest coherency stresses caused in turn by a rather steep density variation at the interface between the phases α and α' .

Figure 1 demonstrates a hitherto unusual behavior of a phase transition. The measured lattice parameters actually do not fit the incoherent phase boundary, depending instead on the chosen sample geometry in a restricted temperature range below T_c . The early spinodal decomposition has been shown to be coherent by the study of the development of density inhomogeneities below T_c , as well as by reversibility measurements above T_c .¹⁷ Thus, the experiments reported here suggest that the coherent phase transition is connected with macroscopic density modes. With

each sample geometry a special precipitation structure of the phases α and α' is uniquely developed.

The shape-dependent phase transition cannot be understood within the framework of a lattice-gas model, where the free energy of the system should be independent of volume in the thermodynamic limit.¹⁸ On the other hand, it has been pointed out recently¹⁴ that in metal-hydrogen systems the requirement of coherency is more stringent than that of a constant and volume-independent chemical potential throughout the crystal. The recent theory of thermodynamics and phase transitions in coherent metal-hydrogen systems,¹⁴ governed by the elastic interaction, indeed yields the unusual features in accordance with our observations: shape-dependent macroscopic modes, without sharp interfaces between the phases α and α' , as well as a strong suppression of critical density fluctuations at the critical point by coherency stresses. The macroscopic shape-dependent modes have been also observed in Gorsky relaxation experiments¹⁹ and have to be clearly distinguished from well-known microscopic or bulk modes in binary alloys with a wavelength much smaller than the sample size.^{20, 21} The latter are insensitive to boundary conditions and their related spinodals and their related spinodals are situated well below the spinodals for macroscopic modes.¹⁴ They have also been seen^{22, 23} at temperatures well below T_c .

It should be noted that there is indirect evidence in all cases of Fig. 1 for the coverage of the α' phase by the α phase even in those situations [1(a) and 1(e)] in which the α' phase is nominally at one surface (or part of one surface). In binary liquids a similiar behavior has been observed,^{24, 25} in which one of the two phases completely wets the other near their critical point, excluding any contact of the enclosed liquid with a third phase. This so-called critical-point wetting has nothing to do with the elastic interaction and coherent phase transition discussed above, but only with the surface free energies of the phases in contact. However, it may be superimposed on the coherent spinodal decomposition and thus, for example, explain the case of Fig. 1(a) in which the mean lattice parameter of the two surfaces seems weighted toward the α boundary as if the α' surface were slightly covered with α . This is currently being examined in further experiments.

We are deeply indebted to H. Wagner, S. C. Moss, and J. W. Cahn for many valuable discussions. We thank the Bundesministerium für

Forschung und Technologie for support of this work. One of us (H.Z.) also acknowledges the support of the U. S. Department of Energy, Office of Basic Energy Sciences.

(a) Present address.

¹G. Alefeld, *Phys. Status Solidi* **32**, 67 (1969).

²R. J. Walter and W. T. Chandler, *Trans. Metall. Soc. AIME* **233**, 762 (1965).

³H. Frieske and E. Wicke, *Ber. Bunsenges. Phys. Chem.* **77**, 48 (1973).

⁴H. Buck and G. Alefeld, *Phys. Status Solidi* **49**, 1 (1976).

⁵C. K. Hall and G. Stell, *Phys. Rev. B* **11**, 224 (1975).

⁶F. D. Manchester, *J. Less Common Metals* **49**, 1 (1976).

⁷T. Fowler and E. A. Guggenheim, *Statistical Thermodynamics* (Cambridge Univ. Press, Cambridge, England, 1956).

⁸T. L. Hill, *Statistical Mechanics* (McGraw-Hill, New York, 1956).

⁹For a review see H. Peisl, in *Topics in Applied Physics*, edited by G. Alefeld and J. Völkl (Springer, Berlin, 1978).

¹⁰H. Metzger, H. Peisl, and H. Wanagel, *J. Phys. F* **6**, 2195 (1976).

¹¹For a homogeneous hydrogen density distribution the relation between the change in lattice constants and the dissolved hydrogen concentration is linear: $c(\text{H/Nb}) = 17.24 \Delta a/a$; H. Pfeiffer and H. Peisl, *Phys. Lett.* **60A**, 363 (1977).

¹²G. Alefeld, *Ber. Bunsenges. Phys. Chem.* **76**, 746 (1972).

¹³G. Alefeld, in *Critical Phenomena*, edited by R. E. Mills and R. I. Jaffee (McGraw-Hill, New York, 1971).

¹⁴H. Wagner and H. Horner, *Adv. Phys.* **23**, 587 (1974).

¹⁵For a review see H. Wagner, in *Topics in Applied Physics*, edited by G. Alefeld and J. Völkl (Springer, Berlin, 1978).

¹⁶H. Zabel and H. Peisl, *Phys. Status Solidi (a)* **37**, K67 (1975).

¹⁷More detailed descriptions of both the coherent and incoherent transition are prepared for publication.

¹⁸M. E. Fisher, *Rep. Prog. Phys.* **30**, 615 (1967).

¹⁹J. Tretkowski, J. Völkl, and G. Alefeld, *Z. Phys. B* **28**, 259 (1977).

²⁰J. W. Cahn, *Acta Metall.* **9**, 795 (1961).

²¹S. C. Moss and B. L. Averbach, in *Proceedings of the Conference on Small Angle Scattering of X-rays*, edited by H. Brunberger (Gordon and Breach, New York, 1967).

²²H. Conrad, G. Bauer, G. Alefeld, T. Springer, and W. Schmatz, *Z. Phys.* **266**, 239 (1974).

²³W. Münzing, thesis, Technical University of München, 1978 (unpublished).

²⁴J. W. Cahn, *J. Chem. Phys.* **66**, 3667 (1977).

²⁵R. B. Heady and J. W. Cahn, *J. Chem. Phys.* **58**, 896 (1973).

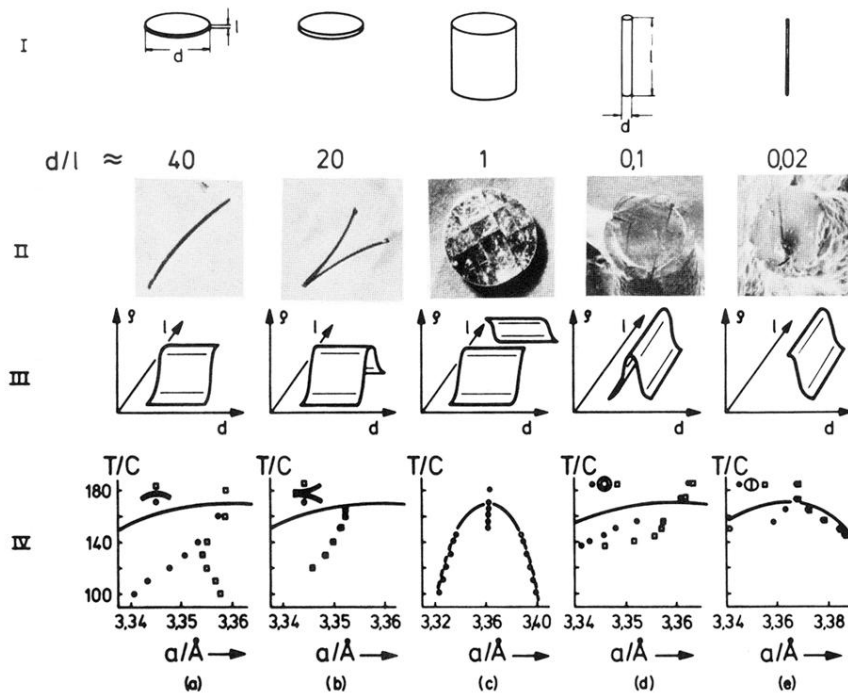


FIG. 1. Sample-shape dependence of macroscopic hydrogen density modes due to coherent phase transition $\alpha-\alpha'$. (a) 0.3-mm-thick disk-shaped single crystal, (b) 0.6-mm-thick disk-shaped single crystal, (c) 2- to 10-mm-thick disks, (d) 1.2-mm-diam wire, (e) 1.76- to 0.25-mm-diam wires. Horizontal designations are (I) initial sample geometry, (II) room-temperature photographs following final measurements [in (IV)], (III) two-dimensional density profiles of the hydrogen fluctuation, (IV) lattice parameter vs temperature taken on different parts of the samples as indicated by the insets. Full lines represent the incoherent $\alpha-\alpha'$ phase boundary.